Research Article

Meiyan Hang, Minghui Jiang*, Junwei Xu, Teng Cheng, Hao Wang and Gangming Zhou

The electrochemical performance and modification mechanism of the corrosion inhibitor on concrete

https://doi.org/10.1515/secm-2021-0037
received April 16, 2021; accepted June 16, 2021

Abstract: The purpose of this study was to solve the chloride corrosion damage problems of the rebar in reinforced concrete structures under the chloride environment. The effects of 1.0% triethanolamine (abbreviated as 1.0% TEA), 1.0% $Ca(NO_2)_2$, and 0.5% TEA + 0.5% $Ca(NO_2)_2$ (abbreviated as 1.0% composite corrosion inhibitor) on the electrochemical performance and modification mechanism of the mortar specimens were investigated by combining macro experiment and microanalysis. The results showed that the electrode potential of the rebar was effectively improved by incorporating the 1.0% composite corrosion inhibitor. This composite corrosion inhibitor displayed the ability to stabilize the electrode potential of the rebar; it also formed a passive film on the surfaces of the rebar, protected the rebar from chloride attack, and achieved satisfactory electrochemical performance. In addition, it could also effectively improve the strength of the mortar specimens and possessed the strong ability to bind chloride ions, thus signifying that it could promote cement hydration and accelerate the formation of cement to form AFt crystals. Therefore, the results of this investigation confirmed that this composite corrosion inhibitor could be effectively used in practical engineering to prevent the corrosion of reinforced concrete structures.

Keywords: corrosion inhibitors, electrochemical performance, modification mechanism

* **Corresponding author: Minghui Jiang,** School of Civil Engineering, Inner Mongolia University of Science and Technology, Baotou, Inner Mongolia, 014010, China, e-mail: 15310062855@163.com
Meiyan Hang, Teng Cheng, Hao Wang: School of Civil Engineering, Inner Mongolia University of Science and Technology, Baotou, Inner Mongolia, 014010, China
Junwei Xu: Haifeng County Investment Holdings Limited, Shanwei City, Guangdong Province, 516400, China
Gangming Zhou: Beijing Tieke Shougang Rail Technology Co., Ltd, Changping district, Beijing, 102206, China

1 Introduction

Reinforced concrete structures are important engineering materials that have been extensively used over the last 100 years due to their convenience of use, low cost, low consumption, and superior properties [1–4]. However, they are easily corroded, particularly under the circumstances of corrosive salt erosion, load action, larger diurnal temperature variation, wet–dry and freeze–thaw cycle, etc. [5]. Due to their tendency to be prone to corrosion damage [6], a large number of durability problems [7] have been encountered, and the service lifespan of reinforced concrete structures does not always meet the specification requirements. It was previously reported that the direct damages caused by the corrosion of reinforced concrete infrastructures in the United States in 2002 resulted in $22.6 billion in damage costs, which not only caused very significant economic losses but also blocked the further promotion of the injured structures [8–13].

Professor Mehta [14] of the University of California clearly stated that rebar corrosion damages were the most important factors affecting the durability of reinforced concrete structures. Researchers have confirmed that rebar corrosion is a major problem and one of the most immediate reasons for the pauperization of reinforced concrete structures and reduction in their durability [15]. Furthermore, chloride presents the most serious detrimental impacts to rebar [16,17], and the presence of chloride has been observed to accelerate the corrosion processes [18,19]. Therefore, it has become an academic issue of widespread concern to researchers. As a result, researchers in the field have attracted widespread attention around the world to solve the problem of preventing the corrosion of rebar caused by chloride.

To date, researchers tend to adopt multiple methods in solving the corrosion problems of rebar and improving the durability of concrete. Such methods have included the incorporation of slag powder, other mineral admixtures, corrosion inhibitors, etc. [20–32]. However, it has

been found that the slag powder decreases the density of the internal concrete, minimizing the strength of the concrete, and reveal the adverse influences on corrosion resistance. Therefore, they cannot be extensively applied because of their negative effects [33,34]. In recent studies, corrosion inhibitors have been widely investigated by researchers due to their simple, economic, efficient, and excellent corrosion resistance characteristics. In the studies conducted by Malik et al. [35], it was found that both the organic inhibitors dimethylethanolamine and triethanolamine (TEA) could reduce the corrosion rates of the rebar, and the corrosion resistance of TEA was observed to be better than that of dimethylethanolamine. In addition, Abd El Haleem et al. [36,37] demonstrated in their research investigations that appropriate amounts of nitrites could thicken the passive film on the surfaces of rebar, thus enhancing their corrosion performance. However, there have been only a few studies regarding the effects of chloride-related rebar. Therefore, it was considered to be of far-reaching significance to carry out in-depth studies regarding the influencing effects of chloride salts on the performance levels of rebar in order to improve the durability of reinforced concrete structures.

In the present study, due to the large dispersion of coarse aggregate, the corrosion state of rebars is nonuniform. Therefore, this study selects mortar specimens instead of concrete specimens to study the chloride corrosion damage problems of reinforced concrete structures under chloride environmental conditions. First, 1.0% TEA, 1.0% $Ca(NO_2)_2$, and 1.0% composite corrosion inhibitors were added into the mortar specimens. In addition, compared with the reference group (without the corrosion inhibitor, denoted 0%), this study investigated the influencing effects of the aforementioned three corrosion inhibitors on the electrochemical properties of the rebar, the strength of the mortar specimens, and the microscopic mechanisms of the mortar specimens in a chloride environment. The results obtained in this study provided important theoretical guidance and technical support for solving the corrosion problems of reinforced concrete structures.

2 Experimental materials and methods

2.1 Raw materials

The P·O 42.5 grade Ordinary Portland cement was used in this study, which was produced by Inner Mongolia Mengxi Co., Ltd. The performance and property parameters of the cement are presented in Table 1. The fineness modulus of the natural river sand used was 2.7, and the mud content was 1.6%. In order to study the influencing effects of the corrosion inhibitor resistance on the rebar mortar specimens, three types of corrosion inhibitors were incorporated into the rebar mortar specimens. The HPB300 plain round rebar was used in this study. Tap water and NaCl solution with a concentration of 3.5% were also utilized for mixing water.

2.2 Experimental methods

2.2.1 Electrochemical measurements in chloride environments

In this study, the HPB300 rebar was processed into a rebar section with diameters of 100 and 7 mm, and then sandpapers were used to polish the surfaces of the rebar in order to achieve a surface roughness of 1.6 μm. Additionally, the rebars were scrubbed with acetone and washed twice with absolute alcohol after drying. The rebar mortar specimens were mixed with a water–cement ratio and a cement–sand ratio of 0.5 and 1:2.5, respectively. The mixing water solution used was a corrosion solution with a chloride concentration of 3.5%. Furthermore, 1.0% TEA, 1.0% $Ca(NO_2)_2$, and 1.0% composite corrosion inhibitors were incorporated into the mortar. The mixed cement mortar was first poured into a mold with 7.5 mm diameter fixed reinforcements at both ends of the mold. The dimensions of the mold were 30 mm × 30 mm × 95 mm.

Table 1: Performance and property parameters of the cement

Fineness (45 μm) (%)	Standard consistency (%)	Specific surface area (m^2/kg)	Setting time (min)		Flexural and compressive strength (MPa)	
			Initial setting	Final setting	3 days	28 days
4.5	27.5	386	135	225	5.0/35.4	8.0/49.8

The rebar–mortar specimens were cured in the mold for a 24 h period. The specimens were then removed from the mold and the curing standards were continued for 28 days. In accordance with the standard technical specifications of corrosion inhibitors used for reinforcing steel in concrete "JT/T 537-2018," a PS-6 steel corrosion measuring instrument was used to test the electrode potentials of the rebar at different time periods in this study.

First, the HPB300 rebar was processed into a rebar section with a diameter of 10 mm. Then, the working face of the rebar was polished step by step with #400–#1200 sandpapers; the copper wire was drilled and welded at the other end and then the epoxy resin was coated on the other side except for the working face. After curing, the epoxy resin was placed in the PVC pipe, and the three corrosion inhibitors were incorporated and vibrated, respectively; finally, the specimens filled with mortar were cured for 24 h. The PVC pipe was removed after standard curing for 28 days. Then, the epoxy resin layer was coated on the side of the specimens again; this was used as the specimen for electrochemical impedance spectroscopy, as shown in Figure 1. In this study, the electrochemical impedance spectroscopy (EIS) of the rebar was investigated according to a standard technical specification for the application of reinforcement corrosion inhibitors "YB/T 9231-2009." The tests were conducted at room temperature of 20 ± 2°C using a Shanghai Chenhua CHI604E electrochemical working instrument. In addition, the electrochemical measurement processes incorporated three electrode systems. For example, the rebar inserted in the specimens was treated as a working electrode, platinum served as a counter electrode, and silver chloride was used as the reference electrode. In the present study, $Ca(OH)_2$ with a chloride concentration of 3.5% was used as the electrolytic solution, and 1.0% TEA, 1.0% $Ca(NO_2)_2$, and 1.0% composite corrosion inhibitors were incorporated into the mortar. Finally, the performance results of the three different types of corrosion inhibitors were investigated.

2.2.2 Mechanical properties of the mortar specimen measurements

The mechanical properties of the mortar specimens were tested according to the standard technical specification "T0506-2005." The mortar specimens cement/ sand/ water were mixed at a ratio of 450:1,350:225. The mixing water was tap water, and 1.0% TEA, 1.0% $Ca(NO_2)_2$, and 1.0% composite corrosion inhibitors were incorporated into the mortar. The mixed cement mortar was poured into a test mold measuring 40 mm × 40 mm × 160 mm, and cured in the mold for 24 h. Then, the specimens were removed from the mold and a standard curing process was carried out. Finally, the flexural strength and compressive strength of the mortar specimens were determined at different ages.

2.2.3 Microstructural analysis

The surface attachments and sludge on the surfaces of the mortar specimens were first cured for 28 days. Then, the specimens were polished using an angular grinder, and 8 mm thin slices were cut in parallel with a cutting machine along the exposed surfaces. Specimens measuring 5 mm × 5 mm × 5 mm were gently tapped with a small hammer. The hydration reactions were terminated using anhydrous ethanol after 7 days. The specimens were exsiccated under vacuum systems for 7 days and sprayed with gold after drying was completed. The 28-day microscopic morphology of each group of specimens was tested using a Sigma 300 scanning electron microscope.

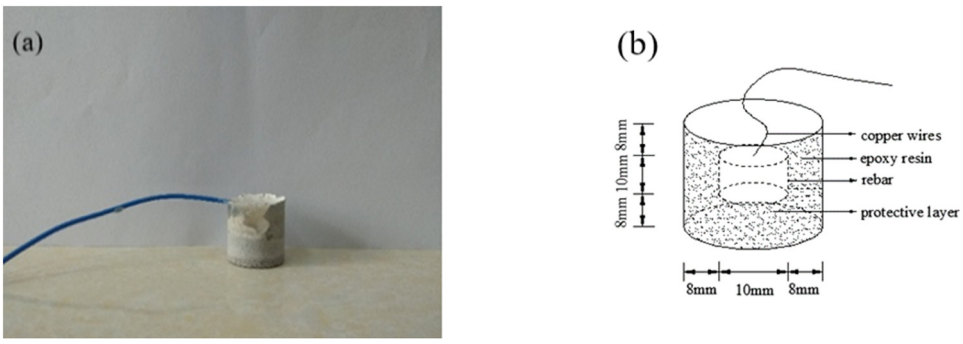

Figure 1: (a) Electrochemical specimen and (b) electrochemical impedance spectroscopy specimen model.

2.2.4 X-ray diffraction analysis

The chemical binding abilities of TEA, $Ca(NO_2)_2$, and composite corrosion inhibitors to chloride ions were investigated by XRD analysis. First, the specimens were extracted from the drill core at the center of the specimen cured for 28 days, and then a grinding machine was used to grind and remove the sand as much as possible. The powder after grinding was screened with a 0.075 mm standard square hole sieve, and the powder with particle sizes less than 0.075 mm was retained. Finally, the XRD analysis was carried out using a D2-PHASER X-ray diffractometer. The system voltage was 40 kV, the current was 20 mA, the scanning rate was 2°/min, and the test range was 10° to 80°(2θ).

3 Results and discussion

3.1 Analysis of the rebar potential

Figure 2 shows the corrosion electrode potentials of the rebar with 0 and 1.0% TEA, 1.0% $Ca(NO_2)_2$, 1.0% composite corrosion inhibitors, and a NaCl solution at a concentration of 3.5%.The influencing effects of corrosion performances and corrosive times of the rebar in the mortar are also displayed. Figure 2 demonstrates that the corrosion potentials of the rebar were inseparably linked to their corrosion resistance levels [38]. It was observed that after being electrified for 2 min, the electrode potentials of the rebar in the reference group rapidly became negative. Then, after 10 min of electrification, the rebar began to corrode. It was also observed that when 1.0% $Ca(NO_2)_2$ inhibitor was added, the rebar decreased rapidly after 10 min of electrification. However, the rebar did not reach a negative potential, and the rebar did not corrode. Also, when 1.0% TEA and 1.0% composite corrosion inhibitors were incorporated, the electrode potentials of the rebar remained stable, which indicated that corrosion inhibitors could effectively prevent the rebar from corroding [39]. It was found that the effects of the composite corrosion inhibitors were more significant. This was due to the fact that the passive film on the surfaces of the rebar remained stable and played important roles in the corrosion resistance processes.

After the electrode potential test was completed, the rebar was removed from the rebar–mortar specimens, and the macroscopic appearances of the rebar of each group are depicted in Figure 3. The figure reveals that the rebar of the reference group was severely corroded, and the rust spot area had covered the whole rebar. However, after the addition of the corrosion inhibitors, the rust spots area on the surface of the rebar decreased significantly and decreased most significantly after incorporation of 1.0% composite corrosion inhibitor. Meanwhile, there was no obvious rust spot on the surface of the rebar, which revealed that the corrosion inhibitor played a very satisfactory role in delaying the corrosion of the rebar, and the inhibitory effect of this composite inhibitor was the most significant. The macroscopic appearance of each group was consistent with the test results of the electrode potential of the rebar.

3.2 Analysis of the electrochemical corrosion performances of the rebar

Figure 4(a)–(c) show the results of the Nyquist, electrochemical impedance spectroscopy, and phase angles of the rebar in the mortar specimens containing 0 and 1.0% TEA, 1.0% $Ca(NO_2)_2$, and 1.0% composite corrosion inhibitors, respectively.

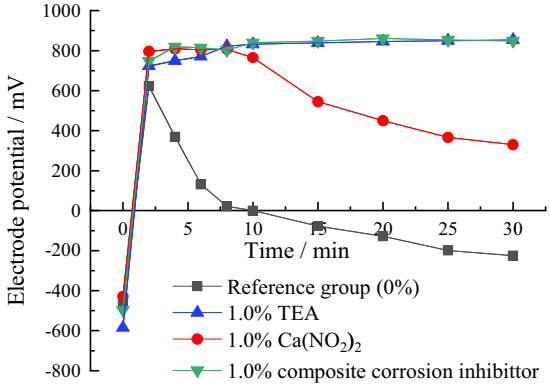

Figure 2: Electrode potentials of the rebar in the mortar specimens.

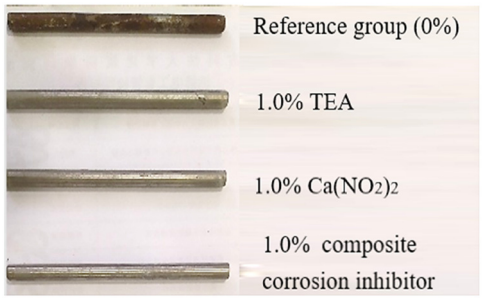

Figure 3: Macroscopic appearance of the rebar.

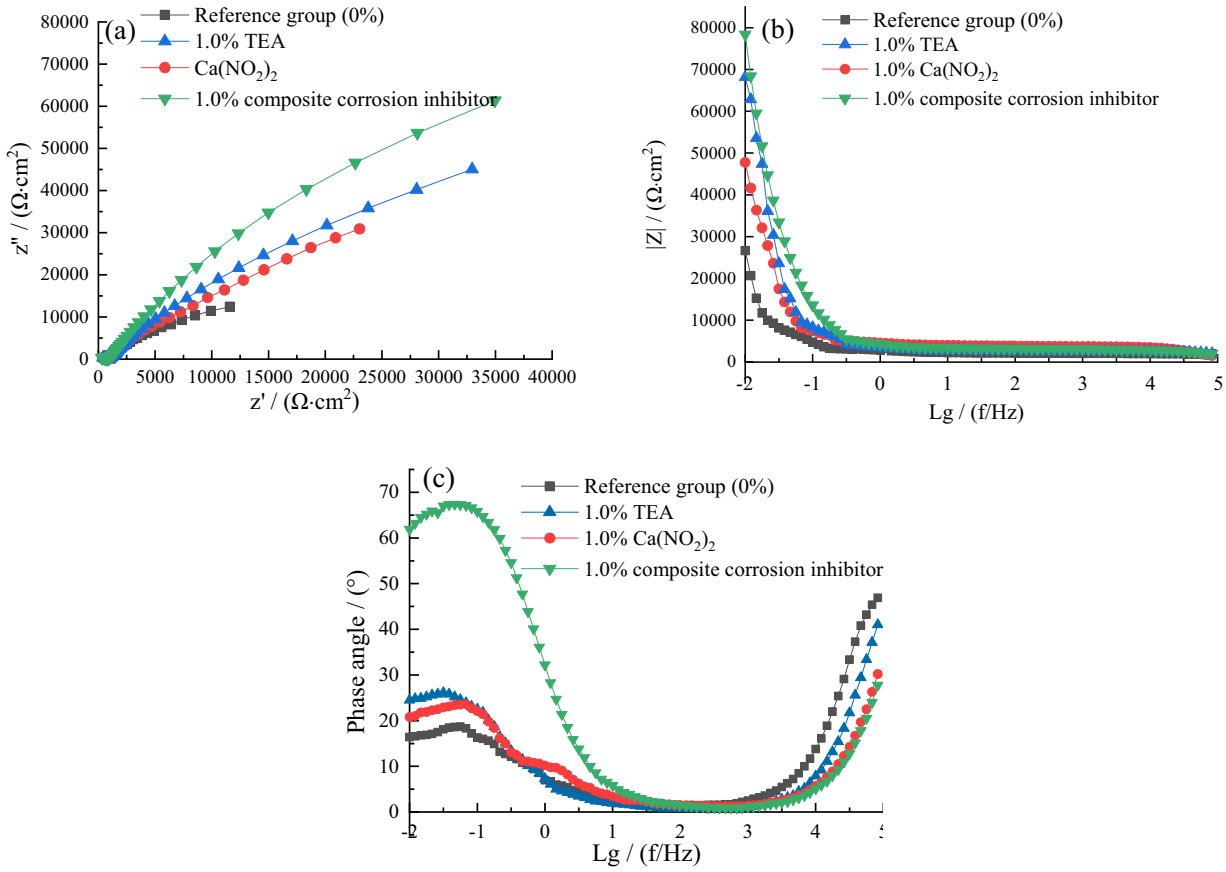

Figure 4: Electrochemical images of the rebar: (a) Nyquist diagram, (b) electrochemical impedance spectroscopy, and (c) phase angles.

Figure 4(a) shows that, compared with the reference group, the capacitive arc radii of the corrosion inhibitor groups were observably multiplied, and the capacitive arc radii of the composite corrosion group were the largest. This indicated that the impedance value might be related to the increase of the surface coverage of corrosion inhibitor molecules of the passivation film, with the molecules of corrosion inhibitors covering the surface of the rebar. Thus, the resistance of Cl^- to the surface of the rebar through the concrete protective layer was higher, which could better protect the rebar. It also hindered the oxidation and reduction reactions on the surface of the rebar and delayed the depassivation time of the passive film on the surface of the rebar. The reason for this could be due to the fact that the addition of the 1.0% composite corrosion inhibitor effectively improved the hydration reaction process of the cement so that the structure was more compact and formed a good protective film on the surface of the rebar. One reason for this was that as TEA contained hydroxyl groups, the corrosion rate of the rebar would gradually decrease as the activity of the hydroxyl groups was greater than that of Cl^-. In addition, the TEA contained N atoms; thus, it would interact with the surface of the rebar to form the passive film and reduce the corrosion rate of the rebar because of the electrostatic effect of N atoms and the common effect of the molecular structure [40]. Another reason was that NO_2^- was a strong oxidizing agent, thus, it could oxidize Fe^{2+} to Fe^{3+}, forming a stable passivation film on the surface of the rebar, and the reaction equations are shown in equations (1)–(4) [41,42], and the modification mechanism model of this corrosion inhibitor is shown in Figure 5.

$$Fe \rightarrow Fe^{2+} + 2e^- \quad (1)$$

$$Ca(NO_2)_2 \rightleftharpoons Ca^{2+} + 2NO_2^- \quad (2)$$

$$H_2O + 1/2O_2 + 2e^- \rightarrow 2OH^- \quad (3)$$

$$Fe^{2+} + 2NO_2^- + 2OH^- \rightarrow \gamma\text{-}Fe_2O_3(\text{Passivation film}) + 2NO\uparrow + H_2O \quad (4)$$

Figure 4(b) shows that a bimodal region related to the double time constant was formed with the incorporation of the corrosion inhibitor; the changes in the electrochemical impedance spectra of the reference group and the groups with 1.0% TEA and 1.0% $Ca(NO_2)_2$ corrosion inhibitors were similar. Also, the electrochemical impedance spectra were very small, which indicated that these two

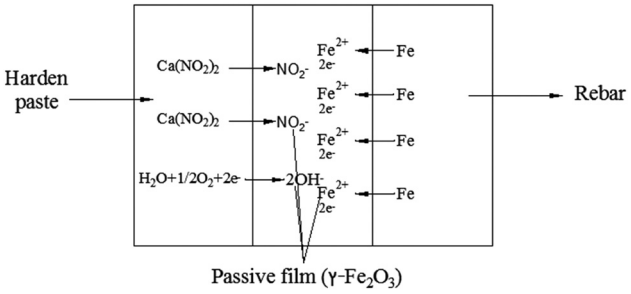

Figure 5: Modification mechanism model of corrosion inhibitors.

types of corrosion inhibitors could not prevent the corrosion of the rebar. Meanwhile, the electrochemical impedance spectra of the rebar in the 1.0% composite corrosion inhibitor were the largest at the lowest frequency, which was approximately 80,000 Ω cm^2. These findings demonstrated that that composite inhibitor had the ability to effectively delay the occurrence of rebar corrosion and continuously form a protective film on the surfaces of the rebar [43]. This resulted in effectively hindering the occurrence of redox reactions on the surfaces of the rebar and reducing the corrosion rates.

Figure 4(c) shows that the corresponding phase angles of the rebar with different corrosion inhibitors in the cement mortar had changed at low frequencies. Meanwhile, the frequencies at the peaks of the phase angles also differ among the three types of inhibitors [44]. It can be seen from the figure that when 1.0% composite corrosion inhibitor was added, the phase angles of the rebar were the largest at the low-frequency levels. At the same time, the frequencies corresponding to the peaks of the phase angles were at the leftmost in the case of 1.0% composite corrosion inhibitor, and the frequencies corresponding to the peaks of the other dosages of corrosion inhibitors had gradually shifted to the right. These results indicated that the passive film on the surfaces of the rebar may have changed under the conditions of incorporating other corrosion inhibitors, and some of the rebars may have become corroded. However, it was confirmed that the composite corrosion inhibitors could effectively protect the rebar and effectively inhibit the occurrence of steel bar corrosion.

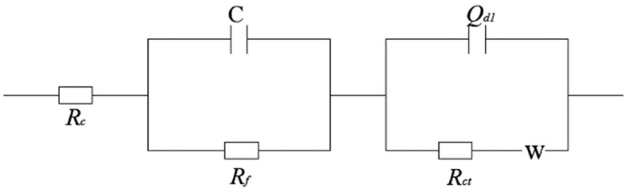

Figure 6: Equivalent circuit model.

The corresponding equivalent circuit diagram was obtained using ZsimpWin software for the EIS data fitting, as shown in Figure 6. The relevant fitting results are detailed in Table 2. The results indicate that the rougher the rebar surfaces, the larger the corresponding Q_{dl} values and the smaller the R_{ct} values. It can be seen in the table that the reference group Q_{dl} was the largest and R_{ct} group was the smallest. These results indicated that the rebar surfaces of the reference group were rough, and rust spots had appeared on the surfaces of the rebar. However, when 1.0% composite corrosion inhibitor was added, the surface charge transfer resistance R_{ct} of the rebars was the largest, along with the R_{ct} values, which were nearly two orders of magnitude higher than that of the reference group. In addition, the Q_{dl} was the smallest, and η had reached a maximum (90.1%). These results indicate that the composite inhibitor displayed good protective effects on the rebar by inhibiting the occurrence of rebar corrosion. These fitting results were consistent with the previous test results.

In the equivalent circuit model, R_s is the solution resistance, Q_{dl} is the double layer capacitance between the surfaces and the solution of the steel bars; R_{cti} is the charge transfer resistance of each group of rebar surfaces, the higher the R_{cti}, the better the inhibition of corrosion inhibitor; and n indicated the ideal degree of fitting for the double-layer capacitance of the corrosion system, while W is the impedance caused by the diffusion of corrosion inhibitor near the film layer.

In Table 2, η represents the inhibition coefficient, which is computed [45] as follows:

$$\eta = \frac{(R_{cti} - R_{ct0})}{R_{cti}} \times 100\% \quad (5)$$

Table 2: Fitting parameters of the rebar impedance with different corrosion inhibitors

Types	R_s (Ω cm^2)	Q_{dl} (μF cm^{-2})	n	R_{cti} (kΩ cm^2)	η (%)
Reference group (0%)	3.08	381.5	0.71	1.80	—
1.0% TEA	2.93	233.9	0.82	5.03	64.2
1.0% $Ca(NO_2)_2$	3.18	195.2	0.81	10.4	82.7
1.0% composite corrosion inhibitor	3.72	54.6	0.85	18.2	90.1

where R_{ct0} is the charge transfer resistance of the reference group.

3.3 Analysis of the flexural and compressive strength levels of the mortar specimens

Figure 7 shows the variations in the flexural and compressive strength levels of the mortar specimens containing different types of corrosion inhibitors. It can be seen in the figure that at each age, the flexural and compressive strengths of the specimens incorporated with TEA and $Ca(NO_2)_2$ corrosion inhibitors were lower than those of the reference group. Meanwhile, the flexural and compressive strengths of the specimens incorporated with the composite corrosion inhibitors were almost higher than those of the reference group at each age. The results demonstrated that the TEA and $Ca(NO_2)_2$ corrosion inhibitors had a negative impact on the strength levels of the specimens, while the composite corrosion inhibitors displayed a positive impact on the strength levels of the specimens. This may be because of the chemical reactions between the compositions of the corrosion inhibitors and the compositions of the cement after the composite corrosion inhibitors were incorporated. During the aforementioned chemical reactions, chemical products were generated; the pores inside the specimens were blocked by crystallization; and the pores were refined or the number of pores was reduced. Therefore, the strength levels of the specimens were increased.

The compressive strength of concrete directly affects its durability in practical engineering. Due to the slow growth rate of the strength of the specimen, the logarithmic function is used to describe the strength growth law of the specimen in this study. Therefore, the origin software was used to establish the growth model of the compressive strength of mortar specimens. The model variable curing age was defined as t ($t \geq 3$ days), and the compressive strength models of the specimens were predicted using equations (6)–(9) as follows:

$$\text{Reference group (0\%): } f_t = \alpha_1 * f_1 * \lg t / \lg 28 \quad (6)$$

$$\text{1.0\% TEA group: } f_t = \alpha_2 * f_2 * \lg t / \lg 28 \quad (7)$$

$$\text{1.0\% } Ca(NO_2)_2 \text{ group: } f_t = \alpha_3 * f_3 * \lg t / \lg 28 \quad (8)$$

$$\text{1.0\% composite corrosion inhibiton: } f_t = \alpha_4 * f_4 * \lg t / \lg 28 \quad (9)$$

where f_t indicates the compressive strength of the specimens on the t-th day; α_i represents the correction coefficient of each group; and f_1, f_2, f_3 and f_4 denote the compressive strengths of the specimens cured for 28 days. Therefore, the compressive strength of each group could be predicted according to equation (3), and the strengths of specimens cured for 3 and 7 days were predicted by this model and compared with the measured values. The error (R) and the square of error (R^2) between the predicted value and the measured value are shown in Table 3. It can be seen from Table 3 that although the errors R and R^2 between the predicted and measured compressive strength of each group of specimens cured for 3 days was less than 0.9, the errors R and R^2 between the predicted and measured compressive strength of each group of specimens cured for 7 days were greater than 0.9, which indicates that these models can better simulate the compressive strength of the specimen after curing for 7 days. Therefore, the compressive strength of each group of specimens after curing for 7 days can be predicted by these compressive strength models.

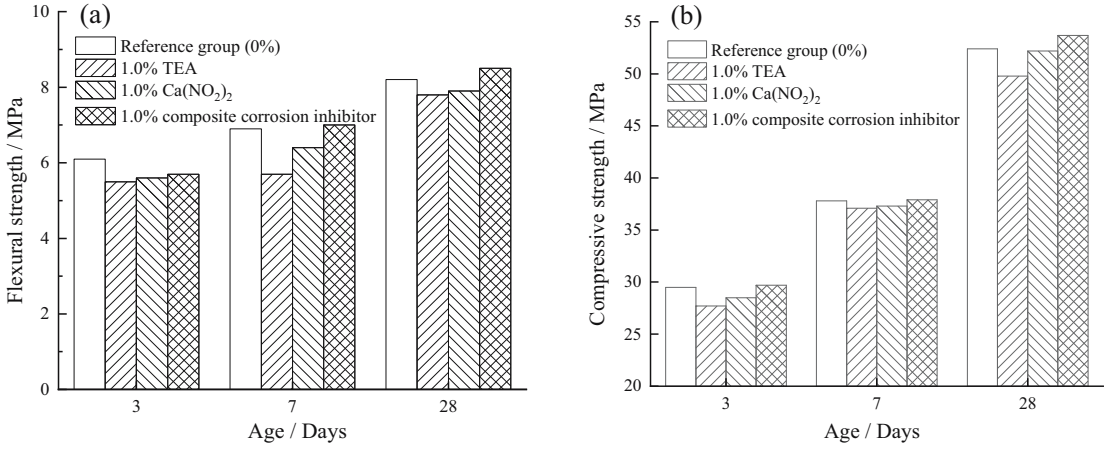

Figure 7: Strength levels of the mortar specimens at different ages: (a) flexural strength and (b) compressive strength.

Table 3: Error statistics between measured and predicted compressive strength of specimens

Types	α_i	3 days		7 days	
		R	R^2	*R*	R^2
Reference group (0%)	1.24770	0.73069	0.53391	0.99005	0.98020
1.0% TEA	1.26109	0.74749	0.55874	0.98853	0.97719
1.0% $Ca(NO_2)_2$	1.23154	0.74368	0.55306	0.99357	0.98718
1.0% composite corrosion inhibitor	1.23146	0.73409	0.55889	0.98142	0.96319

3.4 Micromorphology analysis results

Figure 8 shows the micromorphology images of the mortar specimens containing 1.0% TEA, 1.0% $Ca(NO_2)_2$, and 1.0% composite corrosion inhibitors after curing for 28 days. It can be seen in the figure that the cement hydration processes had generated a large number of hydration products after curing for 28 days. For example, the cement hydration had generated a large number of flocculent C–S–H gels in Group (a). In Group (b), hexagonal plate-like $Ca(OH)_2$ and flocculent C–S–H gels were observed. Group (c) was observed to contain more flocculent and reticular C–S–H gels. Also, a large number of needle-and-stick AFt were generated by the hydration processes in Group (d). The results of this study showed that the addition of different corrosion inhibitors had certain influencing effects on the hydration degrees of the cement. This was mainly due to the different influence of the addition of corrosion inhibitors on the hydrations of C_3A, C_3S, C_4AF, and other minerals as well as the types of hydration products, and the different morphologies of the hydration products of each specimen. This had resulted in different resistance abilities to chloride ion corrosion in the different specimens. In addition, the composite corrosion inhibitors promoted the rapid hydration of C_3A in the cement and accelerated the cement's formation of AFt crystals. At that time, the internal

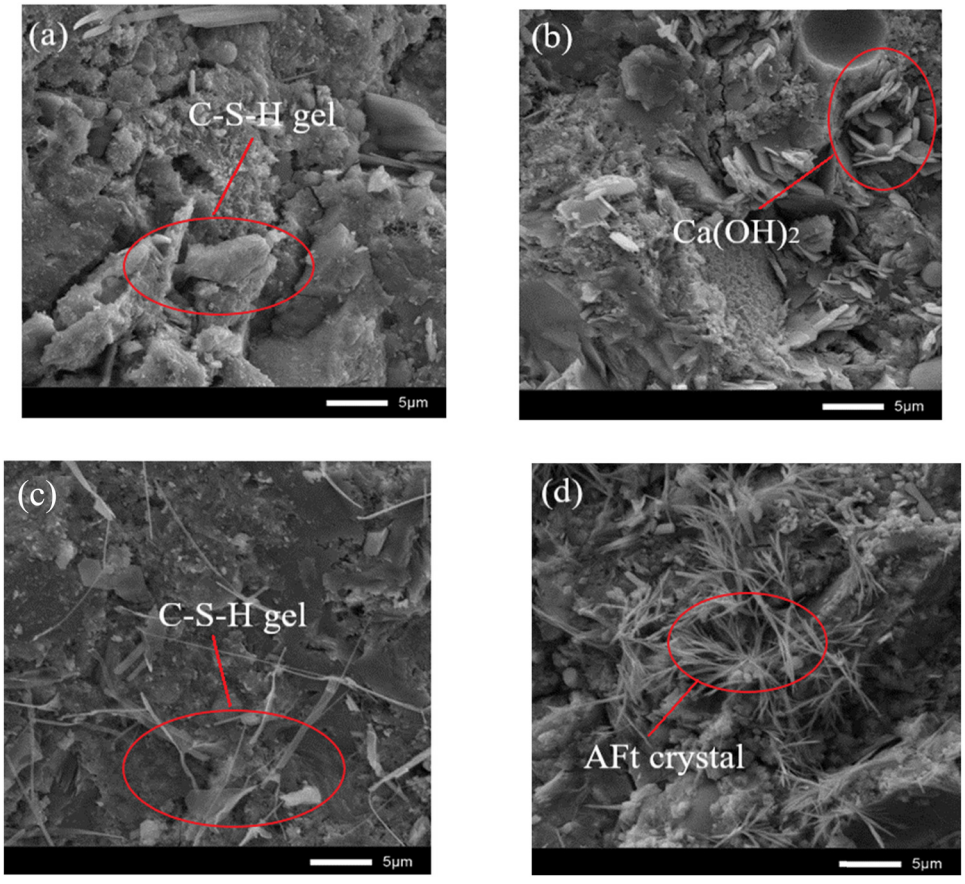

Figure 8: Scanning electron micrographs of the mortar specimens: (a) reference group (0%), (b) 1.0% TEA, (c) 1.0% $Ca(NO_2)_2$, and (d) 1.0% composite corrosion inhibitor.

structures of the mortar were denser, and the anti-chloride corrosion effects of specimens were observed to be better. The reaction equations are as shown in equations (10)–(12):

$$Ca(OH)_2 + 2NaCl \rightleftharpoons Ca^{2+} + Cl^- + 2Na^+ + 2OH^- \quad (10)$$

$$Ca^{2+} + SO_4^{2-} + 2H_2O \rightarrow CaSO_4 \cdot 2H_2O \quad (11)$$

$$3C_3A + 3(CaSO_4 \cdot 2H_2O) + 12H_2O \rightarrow 3C_3A \cdot 3CaSO_4 \cdot 32H_2O \quad (12)$$

3.5 X-ray diffraction analysis

This study aims to study the chemical binding ability of mortar containing different corrosion inhibitors to Cl^-. Figure 9 shows the XRD test results of mortar containing 0%, 1.0% TEA, 1.0% $Ca(NO_2)_2$, and 1.0% composite corrosion inhibitors immersed in 3.5% NaCl solution for 28 days. The reference group showed strong $Ca(OH)_2$, AFt, and weak AFm independent diffraction peaks, and this result indicates that partial AFt was converted to AFm; the reactions are listed in equations (13) and (14). The mortar specimens containing corrosion inhibitors showed not only the independent diffraction peaks of $Ca(OH)_2$ and AFt, but also the independent diffraction peaks of Friedel salt, which demonstrates that corrosion inhibitors can effectively promote the hydration degree of cement and improve the solidification ability of the cement to chloride ions; the reaction equations are shown in equations (15) and (16). Meanwhile, the independent diffraction peaks in the cement mortar containing the composite inhibitor were slightly higher than that in other groups, which indicates that the binding ability of the composite corrosion inhibitor to Cl^- is more significant. The main reason for this is that calcium nitrite can promote the increase of Ca^{2+} concentration, thereby enhancing the formation of $Ca(OH)_2$, and TEA can improve the reaction of C_3A to form AFt.

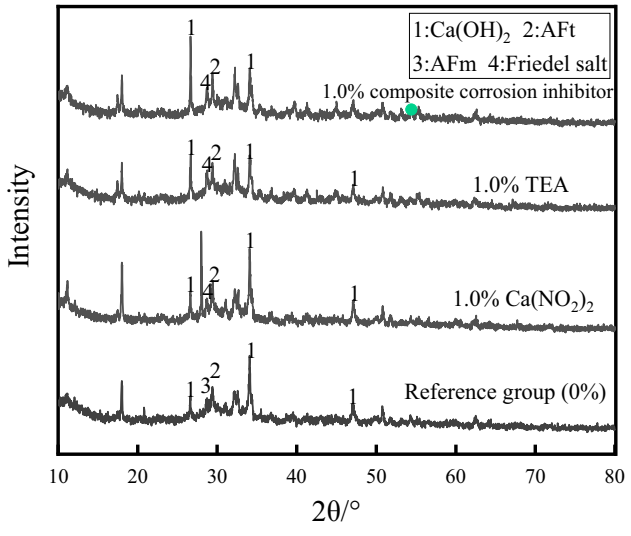

Figure 9: XRD image of mortar specimens cured for 28 days.

$$3C_3A \cdot 6H_2O + 3(CaSO_4 \cdot 2H_2O) + 6H_2O \rightarrow 3C_3A \cdot 3CaSO_4 \cdot 32H_2O \text{ (abbreviated as AFt)} \quad (13)$$

$$C_3A \cdot 3CaSO_4 \cdot 32H_2O + 2(C_3A \cdot 6H_2O) \rightarrow 3(C_3A \cdot CaSO_4 \cdot 12H_2O) \text{ (abbreviated as AFm)} \quad (14)$$

$$Ca(OH)_2 + 2NaCl \rightleftharpoons CaCl_2 + 2NaOH \quad (15)$$

$$3CaO + Al_2O_3 + CaCl_2 + 10H_2O \rightarrow 3CaO \cdot Al_2O_3 \cdot CaCl_2 \cdot 10H_2O \text{ (abbreviated as Friedel salt)} \quad (16)$$

4 Conclusion

In this study, the influencing effects of three corrosion inhibitors (including 1.0% TEA, 1.0% $Ca(NO_2)_2$, and 1.0% composite corrosion inhibitors) on the electrochemical and modification properties of mortar specimens were systematically investigated. Several of the obtained results are compared with the reference group as follows:

(1) This study examined the results of the electrode potential tests of the rebar and observed that the corrosion inhibitors had the ability to improve the electrode potentials of the rebar. In addition, it was found that the $Ca(NO_2)_2$ and composite corrosion inhibitors had successfully stabilized the potentials of the rebar and effectively prevented the rebar from being corroded by chloride. The effects of composite corrosion inhibitors were found to be superior due to the fact that the stability of the passive film on the surface of the rebar could be maintained, which plays an important role in the corrosion resistance of the specimens.

(2) From the electrochemical impedance spectroscopy measurement results, it was determined that composite corrosion inhibitors had effectively delayed the occurrence of corrosion in the rebar and enhanced the formation of a passive film on the surfaces of the rebar. As a result, it was difficult for the chloride ions to contact the rebar surfaces since the passive

film was capable of protecting the reinforced bars from corrosion. This significantly reduced the amount of chloride ions reaching the surfaces of the rebar and provided protection from chloride corrosion. At the same time, the conclusions that were obtained by fitting the data using ZsimpWin software also confirmed the results of the EIS.

(3) From the strength test results, it was determined that composite corrosion inhibitors displayed positive effects on the strength levels of the specimens and had the potential to slightly improve the strength levels of the specimens.

(4) It was concluded from the micromorphology analysis results that the cement hydration process with the composite corrosion inhibitors generated a large number of hydration products, which filled the internal pores and improved the compactness of the specimens. Meanwhile, the composite corrosion inhibitors displayed the ability to accelerate the hydration rates of C_3A and enhance the ability of the cement to form AFt crystals.

(5) From the XRD test results, it was evident that the mortar specimens containing corrosion inhibitors showed the Friedel salt diffraction peak and the diffraction peak of Friedel salt was slightly higher than that of the other groups because the composite corrosion inhibitors have a stronger chemical binding ability to chloride ions and promote the hydration of cement to generate AFt.

Funding information: The study was financially supported by the Natural Science Foundation of Inner Mongolia Province of China (grant no. 2018MS0534) and the Natural Science Foundation of Inner Mongolia (grant no. 2018MS05034).

Author contributions: Conceptualization, Meiyan Hang and Minghui Jiang; methodology, Meiyan Hang, Minghui Jiang and Junwei Xu; investigation, Minghui Jiang, Teng Cheng, Hao Wang and Gangming Zhou; writing—review and editing, Minghui Jiang. All author had read and agreed to the published version of the manuscript.

Conflict of interest: Authors state no conflict of interest.

Data availability statement: All data, models, and code generated or used during the study appear in the submitted article.

References

[1] Liu XH, Ma BG, Tan HB, Gu BQ, Zhang T, Chen P, et al. Effect of aluminum sulfate on the hydration of Portland cement, tricalcium silicate and tricalcium aluminate. Constr Build Mater. 2020;232:117179.

[2] Tan HB, Zhang X, He XY, Guo YL, Deng XF, Su Y, et al. Utilization of lithium slag by wet-grinding process to improve the early strength of sulphoaluminate cement paste. J Clean Prod. 2018;205:536–51.

[3] Gao YL, Qu LC, He B, Dai KM, Fang ZS, Zhu RJ. Study on effectiveness of anti-icing and deicing performance of superhydrophobic asphalt concrete. Constr Build Mater. 2018;191:270–80.

[4] He B, Gao Y, Qu LC, Duan KR, Zhou WJ, Pei GP. Characteristics analysis of self-luminescent cement-based composite materials with self-cleaning effect. J Clean Prod. 2019;225:1169–83.

[5] Xiao JZ, Qiang CB, Nanni A, Zhang KJ. Use of sea-sand and seawater in concrete construction: current status and future opportunities. Constr Build Mater. 2017;155:1101–11.

[6] He ZM, Shen AQ, Guo YC, Lyu ZH, Li DS, Qin X, et al. Cement-based materials modified with superabsorbent polymers: a review. Constr Build Mater. 2019;225:569–90.

[7] Verbruggen H, Terryn H, Graeve ID. Inhibitor evaluation in different simulated concrete pore solution for the protection of steel rebars. Constr Build Mater. 2016;124:887–96.

[8] Flatt RJ, Roussel N, Cheeseman CR. Concrete: an eco-material that needs to be improved. J Eur Ceram Soc. 2012;32(11):2787–98.

[9] Reza SA, Tahir KE, Kambiz R. Permeability properties of self-consolidating concrete containing various supplementary cementitious materials. Constr Build Mater. 2015;79:326–36.

[10] Fu J, Yang F, Guo Z. Facile fabrication of super-hydrophobic filter paper with high water adhesion. Mater Lett. 2019;236:732–5.

[11] Al-Sodani AAK, Maslehuddin M, Al-Amoudi OSB, Saleh TA, Shameem M. Efficiency of generic and proprietary inhibitors in mitigating Corrosion of Carbon Steel in Chloride-Sulfate Environments. Sci Rep. 2018;8(1):11443.

[12] Jin M, Gao S, Jiang LH, Chu HQ, Lu MT, Zhi FF. Degradation of concrete with addition of mineral admixture due to free chloride ion penetration under the effect of carbonation. Corros Sci. 2018;138:42–53.

[13] Loser R, Lothenbach B, Leemann A. Chloride resistance of concrete and its binding capacity – comparison between experimental results and thermodynamic modeling. Cem Concr Compos. 2010;32:34–42.

[14] Mehta PK. Durability-critical issues for the future[J]. Concr Int. 1997;20(7):27–33.

[15] Almusallam AA, Al-Gahtani AS, Aziz AR. Effect of reinforcement corrosion on bond strength. Constr Build Mater. 1996;10:123–9.

[16] Polder RB, Wegen GVD, Breugel KV. Guideline for service life design of structural concrete with regard to chloride induced corrosion-the approach in the Netherlands [J]. Delft; 2010.

[17] Real S, Bogas JA, Ferrer B. Service life of reinforced structural lightweight aggregate concrete under chloride-induced corrosion. Mater Struct. 2017 Apr 1;50(2):101.

[18] Jiang C, Wub Y, Dai M. Degradation of steel-to-concrete bond due to corrosion. Constr Build Mater. 2018;158:1073.
[19] Liang J, Zhu H, Chen L, Han HB, Guo QL, Gao Y, et al. Rebar corrosion investigation in rubber aggregate concrete via the chloride electro-accelerated test. Mater. 2019;12(6):862.
[20] Cook A, Ranke S. Chloride corrosion of steel in concrete. ASTM-STP. 1977;629:51–60.
[21] Abreu AG, Dal Molin DCC. Effect of silica fume addition on electric resistivity of normal strength concrete. IV Congresso Iberoamericano de Patologia das, Construcßoes, VI Congresso de Controle de Qualidade, Anais. 1, 1997. p. 201–8.
[22] Elsener B. Corrosion inhibitors for steel in concrete. Materials Week, International Congress on Advanced Materials, 25–28.9.2000. ICM International Congress Centre Munich. Session E1 Corrosion of Steel in Concrete; 2000.
[23] Al-Amoudi OSB, Maslehuddin M, Lashari AN, Almusallam AA. Effectiveness of corrosion inhibitors in contaminated concrete. Cem Concr Compos. 2003;25(4):439–49.
[24] Söylev TA, Richardson MG. Corrosion inhibitors for steel in concrete: state-of-the-art report. Constr Build Mater. 2006;22(4):609–22.
[25] Tamizhselvi V, Samuel K. Electrochemical investigations to evaluate the performance of inhibitors to control rebar corrosion. Indian Concr Inst J. 2007;8:7–13.
[26] Martínez I, Andrade C, Castellote M. Advancements in non-destructive control of efficiency of electrochemical repair techniques. Corros Eng Sci Technol. 2009;44:108–18.
[27] Plank J, Sakai E, Miao CW, Yu C, Hong JX. Chemical admixtures -chemistry, applications and their impact on concrete microstructure and durability. Cem Concr Res. 2015;78:81–99.
[28] Al-Sodani KAA, Al-Amoudi OSB, Maslehuddin M, Shameem M. Efficiency of corrosion inhibitors in mitigating corrosion of steel under elevated temperature and chloride concentration. Constr Build Mater. 2018;163:97–112.
[29] Sun QL, Liu AR, Guo YZ, Liu F. Effect of new corrosion inhibitor on electrochemical behavior of prestressed steel wire in simulated concrete pore solution. Adv Mat Res. 2014;3226:1390–3.
[30] Fei FL, Hu J, Wei JX. Corrosion performance of steel reinforcement in simulated concrete pore solutions in the presence of imidazoline quaternary ammonium salt corrosion inhibitor. Constr Build Mater. 2014;70:43–53.
[31] Shen L, Jiang H, Cao JD. The effect of electro-migrating 3-Aminopropyltriethoxysilane on the improvement of the reinforced concrete durability. Constr Build Mater. 2019;214:101–10.
[32] Wu M, Ma HF, Shi JJ. Enhanced corrosion resistance of reinforcing steels in simulated concrete pore solution with low molybdate to chloride ratios. Cem Concr Compos. 2020;110:103589.
[33] Aïtcin PC. The durability characteristics of high performance concrete: a review. Cem Concr Compos. 2003;25:409–20.
[34] Cusson D, Hoogeveen T. Internal curing of high performance concrete with pre-soaked fine lightweight aggregate for prevention of autogenous shrinkage cracking. Cem Concr Res. 2008;38:757–65.
[35] Malik AU, Andijani I, Al-Moaili F, Ozair G. Studies on the performance of migratory corrosion inhibitors in protection of rebar concrete in Gulf seawater environment. Cem Concr Compos. 2004;26(3):235–42.
[36] Ramasubramanian M, Haran BS, Popova S, Popov BN, Petrou MF, White RE. Inhibiting action of calcium nitrite on carbon steel rebars. J Mater Civil Eng. 2001;13(1):10–7.
[37] Abd El Haleem SM, Abd El Wanees S, Abd El Aal EE, Diab A. Environmental factors affecting the corrosion behavior of reinforcing steel. IV. Variation in the pitting corrosion current in relation to the concentration of the aggressive and the inhibitive anions. Corros Sci. 2010;52(5):1675–83.
[38] Wang H, Zhang AL, Zhang LC, Liu JZ, Han Y, Shu HB, et al. Study on the influence of compound rust inhibitor on corrosion of steel bars in chloride concrete by electrical parameters. Constr Build Mater. 2020;262:120763.
[39] Nam ND, Hien PV, Hoai NT, Thu VTH. A study on the mixed corrosion inhibitor with a dominant cathodic inhibitor for mild steel in aqueous chloride solution. J Taiwan Inst Chem Eng. 2018;91:556–69.
[40] Liu JP, Chen CC, Cai JS, Liu JZ, Cui G. 1,3-Bis-dibutylamino-propan-2-ol as inhibitor for reinforcement steel in chloride-contaminated simulated concrete pore solution. Mater Corros. 2013;64(12):1075–81.
[41] Anitha R, Chitra S, Hemapriya V, Chung I, Kim S, Prabakaran M. Implications of eco-addition inhibitor to mitigate corrosion in reinforced steel embedded in concrete. Constr Build Mater. 2019;213:246–56.
[42] Zhou Y, Zuo Y. The inhibitive mechanisms of nitrite and molybdate anions on initiation and propagation of pitting corrosion for mild steel in chloride solution. Appl Surf Sci. 2015;353:924–32.
[43] Bairi LR, George RP, Mudali UK. Microbially induced corrosion of D9 stainless steel–zirconium metal waste form alloy under simulated geological repository environment. Corros Sci. 2012;61:19–27.
[44] Cao F, Wei J, Dong J, Ke W. The corrosion inhibition effect of phytic acid on 20SiMn steel in simulated carbonated concrete pore solution. Corros Sci. 2015;100:365–76.
[45] Ismail Y, He P, Nicolas B, Frederic S. Influences of water by cement ratio on mechanical properties of mortars submitted to drying. Cem Concr Res. 2006;36(7):1286–93.